Reduction of deep levels generated by ion implantation into n- and p-type 4H–SiC

Koutarou Kawahara,[1,a)] Jun Suda,[1] Gerhard Pensl,[2] and Tsunenobu Kimoto[1]

[1]*Department of Electronic Science and Engineering, Kyoto University, Katsura, Nishikyo, Kyoto 615-8510, Japan*
[2]*Lehrstuhl für Angewandte Physik, Universität Erlangen-Nürnberg, Staudtstr. 7/A3, D-91058 Erlangen, Germany*

The authors have investigated effects of thermal oxidation on deep levels in the whole energy range of the band gap of 4H–SiC by deep level transient spectroscopy. The deep levels are generated by ion implantation. The dominant defects in n-type samples after ion implantation and high-temperature annealing at 1700 °C are IN3 ($Z_{1/2}$: $E_C - 0.63$ eV) and IN9 ($EH_{6/7}$: $E_C - 1.5$ eV) in low-dose-implanted samples, and IN8 ($E_C - 1.2$ eV) in high-dose-implanted samples. These defects can remarkably be reduced by thermal oxidation at 1150 °C. In p-type samples, however, IP8 (HK4: $E_V + 1.4$ eV) survives and additional defects such as IP4 (HK0: $E_V + 0.72$ eV) appear after thermal oxidation in low-dose-implanted samples. In high-dose-implanted p-type samples, three dominant levels, IP5 (HK2: $E_V + 0.85$ eV), IP6 ($E_V + 1.0$ eV), and IP7 (HK3: $E_V + 1.3$ eV), are remarkably reduced by oxidation at 1150 °C. The dominant defect IP4 observed in p-type 4H–SiC after thermal oxidation can be reduced by subsequent annealing in Ar at 1400 °C. These phenomena are explained by a model that excess interstitials are generated at the oxidizing interface, which diffuse into the bulk region. © *2010 American Institute of Physics*. [doi:10.1063/1.3456159]

I. INTRODUCTION

SiC is a fascinating wide-band gap semiconductor for realizing high-power, high-temperature, and high-frequency devices. Deep levels in semiconductors have several harmful effects such as carrier trapping and reduction in minority carrier lifetime.[1,2] However, the knowledge on the formation of deep levels in ion-implanted SiC is very limited,[3–11] in spite of the fact that ion implantation is an essential process for the fabrication of any kind of SiC devices. In a previous report,[12] deep levels and their depth profiles in N+-, P+-, or Al+-implanted n-/p-type 4H–SiC were systematically investigated, and the dominant defects after 1700 °C annealing have been determined as the IN3 ($Z_{1/2}$: $E_C - 0.63$ eV), IN9 ($EH_{6/7}$: $E_C - 1.5$ eV), IP2 (HS1: $E_V + 0.39$ eV), and IP8 (HK4: $E_V + 1.4$ eV) in low-dose (total dose: 5.6×10^{10} cm^{-2}) implanted samples. In this report, IN8 ($E_C - 1.2$ eV), IP5 (HK2: $E_V + 0.85$ eV), IP6 ($E_V + 1.0$ eV), and IP7 (HK3: $E_V + 1.3$ eV) were observed in high-dose (total dose: 8.0×10^{13} cm^{-2}) implanted samples after annealing at 1700 °C. Because the concentrations of these levels are very high $[(10^{14} - 10^{15})$ cm^{-3} in low-dose samples and $(10^{16} - 10^{17})$ cm^{-3} in high-dose samples], a way to reduce the defects must be established. In this study, the authors attempted to reduce the defects detected in ion-implanted 4H–SiC by thermal oxidation, which is known to be effective for the reduction in deep levels in as-grown 4H–SiC.[13]

II. EXPERIMENTS

The starting materials were N-doped, n-type or Al-doped, p-type 4H–SiC (0001) epilayers with a doping con-

centrations of $(7 - 8) \times 10^{15}$ cm^{-3}. Multiple N+, P+, and Al+ implantation was performed into separate samples at room temperature to form a $(0.7 - 0.8)$ μm deep box profile. The total implanted dose is 5.6×10^{10} cm^{-2} (low-dose condition, $N_I \simeq 7 \times 10^{14}$ cm^{-3}) or 8.0×10^{13} cm^{-2} (high-dose condition, $N_I \simeq 1 \times 10^{18}$ cm^{-3}). The detailed implantation conditions are described in a previous report.[12] Figure 1 shows the depth profiles of the implanted N atoms simulated by a TRIM code. High-dose condition is generally used to form pn junctions. Under low-dose condition, the concentration of implanted impurities is lower than the doping level of the epilayers. Since the samples keep the original conduction type (n- or p-type), deep levels located in the upper half of the band gap can be monitored by using n-type epilayers, irrespective of the implanted species, and in the same way, deep
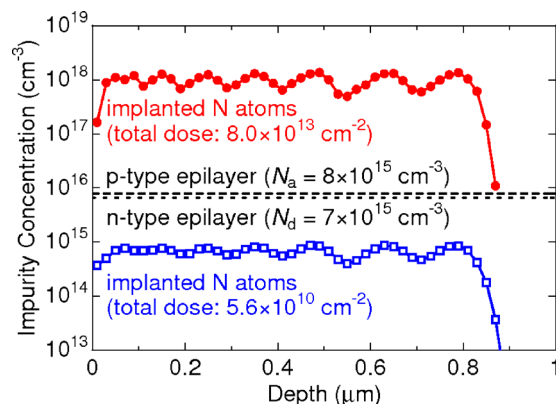

FIG. 1. (Color online) Depth profiles of implanted N atoms simulated by TRIM code (closed circles: high-dose implanted N atoms, squares: low-dose-implanted N atoms, and dotted/broken lines: doping levels in n-/p-type starting materials).

---

a)Electronic mail: kawahara@semicon.kuee.kyoto-u.ac.jp.
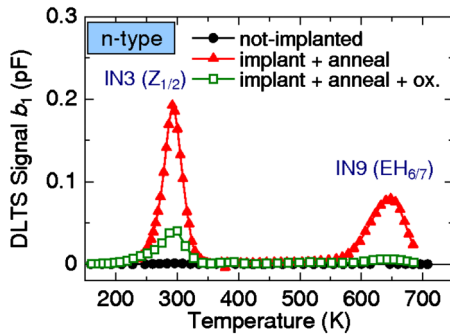
108, 033706-1

FIG. 2. (Color online) DLTS spectra of not-implanted (closed circles) and low-dose Al$^+$-implanted, n-type 4H–SiC after 1700 °C annealing (closed triangles) and the after annealing plus oxidation at 1150 °C (squares).

levels in the lower half of the band gap by using p-type materials. Postimplantation annealing was carried out at 1700 °C for 30 min. For the deep level transient spectroscopy (DLTS) measurements, Ni and Ti were employed as Schottky contacts (typical diameter: 1 mm) on n- and p-type samples, respectively. A period width of 0.205 s was employed for all DLTS measurements performed in this study. A typical reverse bias is −1 V (for n-type) or 1 V (for p-type) and filling pulse voltage is 0 V. After the first DLTS measurement, all the contacts were removed and thermal oxidation was performed in dry O$_2$ at 1150 °C for 2 h, by which 25 nm-thick SiO$_2$ is formed. After removing the oxide, new Schottky contacts were prepared and the DLTS measurements were repeated.

III. RESULTS AND DISCUSSION

A. Deep levels detected in n-type materials

Figure 2 shows the DLTS spectra obtained from low-dose-Al$^+$ implanted, n-type 4H–SiC after annealing at 1700 °C (closed triangles) and after annealing plus oxidation (squares). DLTS spectrum obtained from not-implanted sample is also shown by closed circles, in which well known deep levels, Z$_{1/2}$ (Ref. 3) ($E_C - 0.63$ eV) and EH$_{6/7}$ (Ref. 14) ($E_C - 1.6$ eV), are detected at the concentration of $(1-2) \times 10^{13}$ cm^{-3}. After the implantation, a high density of traps [IN3 (Z$_{1/2}$) and IN9 (EH$_{6/7}$)] is generated. The defect concentrations (Z$_{1/2}$: 3×10^{15} cm^{-3}) are higher than the concentration of the implanted ions (about 7×10^{14} cm^{-3}) after 1700 °C annealing. These thermally stable traps (Z$_{1/2}$ and EH$_{6/7}$) are dramatically reduced by the subsequent oxidation. It should be noted that an only 15 nm-thick surface layer was
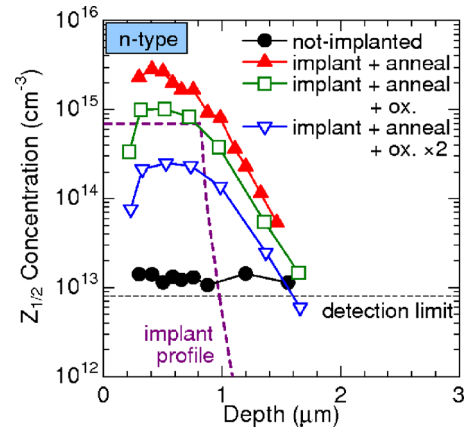

FIG. 3. (Color online) Depth profiles of the Z$_{1/2}$ center observed in not-implanted (closed circles) and Al$^+$-implanted, n-type 4H–SiC after 1700 °C annealing (closed triangles) and after the annealing plus oxidation at 1150 °C (squares and inverse triangles).

consumed by the oxidation, and the main body of the implanted region, (0.7−0.8) μm, remains. The parameters of the deep levels detected in low-dose ion-implanted n-type 4H–SiC are summarized in Table I. The remarkable reduction in these defects by thermal oxidation agrees with our recent results obtained for as-grown 4H–SiC.[13] According to the literature,[15,16] the origin of the Z$_{1/2}$ and EH$_{6/7}$ may be a defect containing a carbon vacancy. These carbon vacancies might be occupied by C or Si interstitials (C$_I$ or Si$_I$) generated by the thermal oxidation.[13] The literature suggests the generation of C$_I$ at the SiO$_2$/SiC interface during oxidation,[17,18] which also supports this model.

Figure 3 shows the depth profiles of the Z$_{1/2}$ defect observed in low-dose-Al$^+$ implanted, n-type 4H–SiC after 1700 °C annealing (closed triangles) and after annealing plus oxidation (squares and inverse triangles). The depth profiles were measured by changing the bias voltage (both pulse voltage and reverse voltage) in the DLTS measurements, by which the emission from different zones of the space charge region can be monitored. Here, ox. ×2 means two successive oxidations at 1150 °C for 2 h. The Z$_{1/2}$ center in not-implanted sample (closed circles) is uniformly distributed at the concentration of $(1-2) \times 10^{13}$ cm^{-3} along the depth. The Z$_{1/2}$-profile extended to a depth of about 1.5 μm by the Al$^+$-implantation and annealing at 1700 °C for 30 min, which significantly decreases after every oxidation. The Z$_{1/2}$ concentration is reduced from about 3×10^{15} cm^{-3} (closed triangles) to 1×10^{15} cm^{-3} (squares) by the first oxidation,

TABLE I. Energy positions and capture cross-sections of deep levels observed in low-dose ion-implanted, n-type 4H–SiC (σ: the capture cross-section, N_T: the concentration of traps at about 0.5 μm from the surface in the Al$^+$-implanted SiC before and after oxidation at 1150 °C for 2 h).

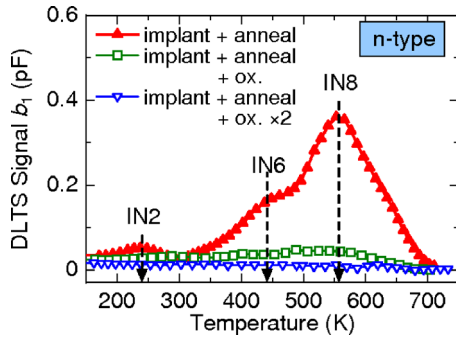| Label	$E_C - E_T$ (eV)	σ (cm^2)	N_T (cm^{-3}) Before ox.	After ox.	After ox. ×2	Corresponding center
IN3	0.63	10^{-14}	3×10^{15}	1×10^{15}	2×10^{14}	Z$_{1/2}$ [a]
IN9	1.5	10^{-14}	8×10^{14}	5×10^{14}	2×10^{14}	EH$_{6/7}$ [b]

[a]Reference 3.
[b]Reference 14.

FIG. 4. (Color online) DLTS spectra of high-dose P$^+$-implanted, n-type 4H–SiC after 1700 °C annealing (closed triangles) and after the annealing plus oxidation at 1150 °C (squares and inverse triangles).
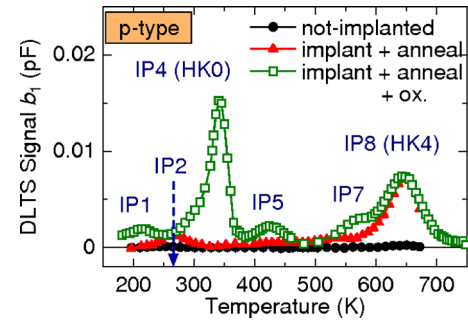

FIG. 5. (Color online) DLTS spectra of not-implanted (closed circles) and low-dose Al$^+$-implanted, p-type 4H–SiC after 1700 °C annealing (closed triangles) and after the annealing plus oxidation at 1150 °C (squares).

and to 3×10^{14} cm^{-3} (inverse triangles) by the second oxidation at a depth of about 0.5 μm. The same phenomenon was observed for EH$_{6/7}$ (not shown), which indicates that all the major deep levels observed in ion-implanted n-type 4H–SiC can be remarkably reduced by the oxidation, when the implanted dose is relatively low. The corresponding deep levels in samples implanted with the other species (N$^+$, P$^+$) showed a similar behavior.

Figure 4 shows the DLTS spectra obtained from high-dose P$^+$-implanted, n-type 4H–SiC after annealing at 1700 °C (closed triangles) and after annealing plus oxidation (squares and inverse triangles). In the implanted sample after annealing at 1700 °C, IN2 ($E_C - 0.30$ eV), IN6 ($E_C - 1.0$ eV), and IN8 ($E_C - 1.2$ eV) are observed at significantly high concentrations (IN8: $\sim 1 \times 10^{17}$ cm^{-3}). The IN2 center may be assigned to ID$_8$ detected in (Ti$^+$, V$^+$, or Al$^+$)-implanted n-type 4H–SiC after annealing at 1700 °C for 30 min.[3,4] The parameters of the deep levels detected in high-dose ion-implanted, n-type 4H–SiC are summarized in Table II. Although the peak labeled IN8 is too broad to be a single level, other levels cannot be resolved due to severe overlapping. Note that all defects including the dominant level of the IN8 center remarkably decrease after every oxidation. The concentration of the IN8 center after the first/second oxidation (squares/inverse triangles in Fig. 4) is $\sim 2 \times 10^{16}$ cm^{-3}/lower than 4×10^{15} cm^{-3}.

B. Deep levels detected in p-type materials

Figure 5 shows the DLTS spectra obtained from low-dose Al$^+$-implanted, p-type 4H–SiC after annealing at 1700 °C (closed triangles) and subsequent oxidation (squares). DLTS spectrum obtained from not-implanted sample is also shown by closed circles, in which D (Ref. 4) ($E_C - 0.63$ eV) and IP8 [HK4 (Ref. 19): $E_V + 1.4$ eV] centers are detected at the concentration of about 3×10^{12} cm^{-3} and 3×10^{13} cm^{-3}, respectively. After the implantation, two traps, IP2 [HS1 (Refs. 15 and 20): $E_V + 0.39$ eV] and IP8 (HK4), are dominant. In contrast to n-type samples, several levels, IP1 ($E_V + 0.30$ eV), IP4 ($E_V + 0.72$ eV), IP5 ($E_V + 0.85$ eV), and IP7 ($E_V + 1.3$ eV), are generated by the oxidation of the implanted p-type samples. The IP1, IP4, IP5, and IP7 centers may be the same defects as the UK1, HK0, HK2, and HK3 centers previously detected in p-type 4H–SiC.[19] The UK1 and HK0 centers were observed in irradiated samples after annealing at 950 °C, while the HK2 and HK3 centers were first detected in as-grown samples.[19] The HK0 center is also generated by reactive ion etching followed by thermal oxidation.[19] Because these four levels were also observed in not-implanted samples after thermal oxidation (not shown), these levels will originate from intrinsic defects (e.g., C or Si interstitial(s), Si antisite), which do not contain the implanted species. The parameters of the deep levels detected in low-dose-ion-implanted p-type 4H–SiC are summarized in Table III.

Figure 6 shows the depth profiles of the IP4 (HK0) and IP8 (HK4) centers observed in low-dose-Al$^+$-implanted p-type 4H–SiC after 1700 °C annealing (HK4: closed triangles) and subsequent oxidation (HK4: squares, HK0: rhombuses). The HK0 center was generated especially near the surface ($>10^{14}$ cm^{-3}) after oxidation. The HK0 center is discussed in the next subsection. Before oxidation, the HK4 center existed only near the surface reaching a depth of about 0.4 μm. After the oxidation, however, the HK4 profile was

TABLE II. Energy positions and capture cross-sections of deep levels observed in high-dose ion-implanted, n-type 4H–SiC (σ: the capture cross-section, N_T: the concentration of traps at about 0.02 μm from the surface in the P$^+$-implanted SiC before and after oxidation at 1150 °C for 2 h).

Label	$E_C - E_T$ (eV)	σ (cm^2)	N_T (cm^{-3}) Before ox.	After ox.	After ox. $\times 2$	Corresponding center
IN2	0.30	10^{-18}	1×10^{16}	$< 6 \times 10^{15}$	$< 2 \times 10^{15}$	ID$_8$ [a]
IN6	1.0	10^{-15}	5×10^{16}	$< 2 \times 10^{16}$	$< 7 \times 10^{15}$	
IN8	1.2	10^{-15}	1×10^{17}	$< 2 \times 10^{16}$	$< 4 \times 10^{15}$	

[a]References 3 and 4.

TABLE III. Energy positions and capture cross-sections of deep levels observed in low-dose ion-implanted, p-type 4H–SiC (σ: the capture cross-section, N_T: the maximum concentration of traps at $0.1-0.6$ μm from the surface in the Al$^+$-implanted SiC before and after oxidation at 1150 °C for 2 h).

Label	$E_T - E_V$ (eV)	σ (cm^2)	N_T (cm^{-3}) Before ox.	After ox.	Corresponding center
IP1	0.30	10^{-18}	Not observed	2×10^{13}	UK1[a]
IP2	0.39	10^{-18}	2×10^{13}	$<2 \times 10^{13}$	HS1[b,c]
IP4	0.72	10^{-16}	6×10^{12}	3×10^{14}	HK0[a]
IP5	0.85	10^{-16}	Not observed	3×10^{13}	HK2[a]
IP7	1.3	10^{-14}	1×10^{13}	6×10^{13}	HK3[a]
IP8	1.4	10^{-16}	2×10^{14}	2×10^{14}	HK4[a]

[a]Reference 19.
[b]Reference 15.
[c]Reference 20.

extended to a depth of about 0.8 μm while HK4 did not increase near the surface. The depth profile of the HK4 center is very similar to that of the HK0 center after oxidation, which indicates that the origin of the two levels may contain the same defect. The corresponding deep levels in samples implanted with the other species (N$^+$,P$^+$) showed a similar behavior.

Figure 7 shows the DLTS spectra obtained from high-dose Al$^+$-implanted, p-type 4H–SiC after annealing at 1700 °C (closed triangles) and after annealing plus oxidation (squares). In the implanted sample after annealing, IP5 (E_V +0.85 eV), IP6 (E_V+1.0 eV), IP7 (E_V+1.3 eV), and IP9 (E_V+1.5 eV) are observed at high concentrations (IP5: 1 $\times 10^{16}$ cm^{-3}). Other levels, which cannot be resolved due to the overlapping of DLTS peaks, should also exist in this high-dose-implanted p-type sample. However, all these defects decrease by thermal oxidation (IP5: 6×10^{15} cm^{-3}). The parameters of the deep levels detected in high-dose Al$^+$-implanted, p-type 4H–SiC are summarized in Table IV.

IV. DISCUSSION

All the levels detected in low-dose implanted 4H–SiC may originate from intrinsic defects as discussed in a previous report.[12] In high-dose implanted, n-type samples, three major defects (IN2, IN6, and IN8) were always observed irrespective of the implanted species (N and P), indicating intrinsic defects. However, it is difficult to judge whether defects containing the implanted species do exist (or not) in high-dose implanted, n-type samples due to the severe overlapping of DLTS peaks. The concentration of deep levels in high-dose implanted, n-type 4H–SiC ($\sim 10^{17}$ cm^{-3}) is about two orders of magnitude higher than that in the low-dose, n-type 4H–SiC ($\sim 10^{15}$ cm^{-3}). Also in p-type samples, the trap concentration after high-dose ion implantation ($\sim 10^{16}$ cm^{-3}) is about two orders of magnitude higher than that after low-dose implantation ($\sim 10^{14}$ cm^{-3}). The concentration of the implanted species is about 1×10^{18} cm^{-3} in high-dose implanted samples and 7×10^{14} cm^{-3} in low-dose implanted samples. Under high-dose condition, a standard condition for forming pn junctions, the concentration of deep levels reaches above 10% of the doping concentration leading to high compensation. Under low-dose condition corresponding to the "implanted-tail" region, where minority carriers are injected under forward bias, the concentration of deep levels exceed that of implanted atoms. Such great amount of deep levels in the implanted-tail region should lead to short lifetimes.

While almost all the deep levels generated by implantation in the upper half of the band gap can greatly be reduced by thermal oxidation, the IP4 (HK0) center (E_V+0.72 eV) is
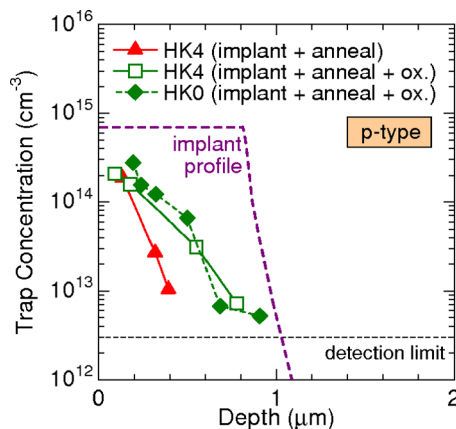

FIG. 6. (Color online) Depth profiles of the IP4 (HK0) and IP8 (HK4) centers observed in low-dose Al$^+$-implanted, p-type 4H–SiC after 1700 °C annealing (HK4: closed triangles) and subsequent oxidation at 1150 °C (HK4: squares, HK0: rhombuses).
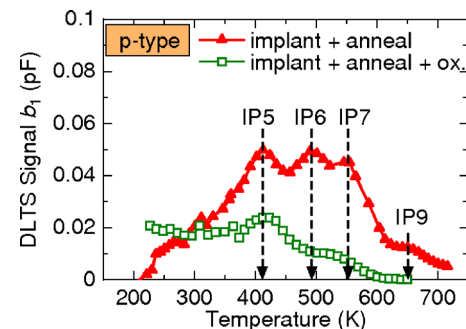

FIG. 7. (Color online) DLTS spectra of high-dose Al$^+$-implanted, p-type 4H–SiC after 1700 °C annealing (closed triangles) and after the annealing plus oxidation at 1150 °C (squares).

TABLE IV. Energy positions and capture cross-sections of deep levels observed in high-dose Al$^+$-implanted, p-type 4H–SiC (σ: the capture cross-section, N_T: the concentration of traps at about 0.02 μm from the surface in the SiC before and after oxidation at 1150 °C for 2 h).

Label	$E_T - E_V$ (eV)	σ (cm^2)	N_T (cm^{-3}) Before ox.	After ox.	Corresponding center
IP5	0.85	10^{-16}	1×10^{16}	6×10^{15}	HK2[a]
IP6	1.0	10^{-14}	1×10^{16}	$<4 \times 10^{15}$	
IP7	1.3	10^{-14}	1×10^{16}	$<3 \times 10^{15}$	HK3[a]
IP9	1.5	10^{-15}	6×10^{15}	$<7 \times 10^{13}$	

[a]Reference 19.

generated by the oxidation. In order to fabricate high-performance SiC devices, the thermal oxidation will be effective but an additional treatment for reducing the HK0 center must be conducted. The origin of the HK0 center may be a C_I- or Si_I-related defect generated by thermal oxidation, based on the following results.[21] It has been reported that an interfacial transition layer is observed at the SiO_2/SiC interface by secondary ion mass spectrometry (SIMS).[22] At the SiO_2/SiC interface, a C-rich region was also observed by Electron Energy Loss Spectroscopy (EELS).[23,24] In addition, it is predicted that carbon clusters $[(C_I)_2]$ are formed at the interface during thermal oxidation from a density functional theory.[17] Furthermore, a model considering emission of C_I and Si_I from the SiO_2/SiC interface during oxidation can well simulate the experimental oxidation rate of SiC.[18] Since the HK0 center is always generated near the SiO_2/SiC interface by thermal oxidation, the HK0 center may contain C_I or Si_I.

In a previous report,[19] the authors showed that the HK0 center can almost be annealed out by thermal treatment in Ar at 1550 °C for 30 min. This high-temperature treatment, however, is not always compatible with the real device processing. For example, after gate oxidation for metal-oxide-semiconductor devices, by which the HK0 center is generated, thermal treatment above 1400 °C will cause severe degradation/decomposition of SiO_2.

To investigate the thermal stability of the HK0 center, the authors annealed the oxidized samples (not-implanted) at 1300 or 1400 °C in N_2 ambient. The oxidation was performed in N_2O diluted with N_2 at 1300 °C for 30 min resulting in an SiO_2 thickness of 4 nm. The observed defects are the same as the defects detected in the sample oxidized at 1150 °C in O_2 ambient. Figure 8 shows the depth profiles of the HK0 center observed in p-type 4H–SiC after oxidation (closed circles) and after oxidation and annealing (triangles: at 1300 °C for 30 min, closed squares: at 1300 °C for 300 min, inverse triangles: at 1400 °C for 30 min). The HK0 center was reduced in a depth >0.4 μm and also in the near-surface region by annealing at 1300 °C for 30 min. C_I and Si_I generated by oxidation may diffuse toward a deeper region (toward the substrate) and perhaps also toward the surface during the annealing. This may be the reason why the HK0 center is reduced especially in a deep region and a near-surface region. When the annealing time is extended (closed squares in Fig. 8) or the annealing temperature is higher (inverse triangles in Fig. 8), the HK0 center almost disappears, also near the surface (~ 0.4 μm).

V. CONCLUSION

Our DLTS investigations on implanted SiC have shown that thermal oxidation of low-dose ion-implanted 4H–SiC leads to a remarkable reduction in the IN3 ($Z_{1/2}$) and IN9 ($EH_{6/7}$) centers in the upper half of the band gap (the $Z_{1/2}$ concentration at a depth of 0.4 μm varies from 3×10^{15} to 2×10^{14} cm^{-3}), and, on the other hand, to the generation of several deep defects such as the IP4 (HK0) center (concentration at a depth of 0.2 μm: $\sim 3 \times 10^{14}$ cm^{-3}) in the lower half of the band gap. It is speculated that excess interstitials are generated at the oxidizing interface and diffuse into the bulk region. The reduction in the $Z_{1/2}$ and $EH_{6/7}$ by thermal oxidation may be explained by our proposal that these defects, which may be V_C-related,[15,16] are occupied by interstitials. The dominant defects in high-dose ion-implanted 4H–SiC, IN8, IP5, IP6, and IP7, also drastically decrease by thermal oxidation (IN8 concentration: from 1×10^{17} to 2×10^{16} cm^{-3}). The origin of HK0 generated by thermal oxidation may be an interstitial-related defect, which can diffuse and decrease by annealing at temperatures above 1300 °C. Consequently, in order to realize high-performance SiC devices, ion-implanted 4H–SiC should be oxidized and subsequently annealed above 1300 °C.
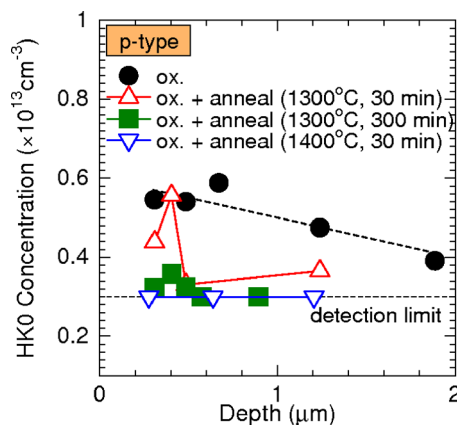

FIG. 8. (Color online) Depth profiles of the IP4 (HK0) center observed in p-type 4H–SiC after oxidation at 1300 °C (closed circles) and after oxidation and annealing (triangles: at 1300 °C for 30 min, closed squares: at 1300 °C for 300 min, inverse triangles: at 1400 °C for 30 min).

ACKNOWLEDGMENTS

[1] K. Danno, D. Nakamura, and T. Kimoto, Appl. Phys. Lett. **90**, 202109 (2007).

[2] P. B. Klein, J. Appl. Phys. **103**, 033702 (2008).

[3] T. Dalibor, G. Pensl, H. Matsunami, T. Kimoto, W. J. Choyke, A. Schöner, and N. Nordell, Phys. Status Solidi A **162**, 199 (1997).

[4] T. Troffer, M. Schadt, T. Frank, H. Itoh, G. Pensl, J. Heindl, H. P. Strunk, and M. Maier, Phys. Status Solidi A **162**, 277 (1997).

[5] R. Kumar, J. Kozima, and T. Yamamoto, Jpn. J. Appl. Phys., Part 1 **39**, 2001 (2000).

[6] S. Mitra, M. V. Rao, N. Papanicolaou, K. A. Jones, M. Derenge, O. W. Holland, R. D. Vispute, and S. R. Wilson, J. Appl. Phys. **95**, 69 (2004).

[7] G. Alfieri, E. V. Monakhov, B. G. Svensson, and A. Hallén, J. Appl. Phys. **98**, 113524 (2005).

[8] Y. Negoro, T. Kimoto, and H. Matsunami, J. Appl. Phys. **98**, 043709 (2005).

[9] M. Canino, A. Castaldini, A. Cavallini, F. Moscatelli, R. Nipoti, and A. Poggi, Mater. Sci. Forum **527–529**, 811 (2006).

[10] G. Alfieri and T. Kimoto, J. Appl. Phys. **101**, 103716 (2007).

[11] J. Wong-Leung and B. G. Svensson, Appl. Phys. Lett. **92**, 142105 (2008).

[12] K. Kawahara, G. Alfieri, and T. Kimoto, J. Appl. Phys. **106**, 013719 (2009).

[13] T. Hiyoshi and T. Kimoto, Appl. Phys. Express **2**, 041101 (2009).

[14] C. Hemmingsson, N. T. Son, O. Kordina, J. P. Bergman, E. Janzén, J. L. Lindström, S. Savage, and N. Nordell, J. Appl. Phys. **81**, 6155 (1997).

[15] L. Storasta, J. P. Bergman, E. Janzén, A. Henry, and J. Lu, J. Appl. Phys. **96**, 4909 (2004).

[16] K. Danno and T. Kimoto, J. Appl. Phys. **100**, 113728 (2006).

[17] J. M. Knaup, P. Deák, T. Frauenheim, A. Gali, Z. Hajnal, and W. J. Choyke, Phys. Rev. B **71**, 235321 (2005).

[18] Y. Hijikata, H. Yaguchi, and S. Yoshida, Appl. Phys. Express **2**, 021203 (2009).

[19] K. Danno and T. Kimoto, J. Appl. Phys. **101**, 103704 (2007).

[20] L. Storasta, F. H. C. Carlsson, S. G. Sridhara, J. P. Bergman, A. Henry, T. Egilsson, A. Hallén, and E. Janzén, Appl. Phys. Lett. **78**, 46 (2001).

[21] T. Hiyoshi and T. Kimoto, Appl. Phys. Express **2**, 091101 (2009).

[22] T. Kimoto, Y. Kanzaki, M. Noborio, H. Kawano, and H. Matsunami, Jpn. J. Appl. Phys., Part 1 **44**, 1213 (2005).

[23] K. C. Chang, N. T. Nuhfer, L. M. Porter, and Q. Wahab, Appl. Phys. Lett. **77**, 2186 (2000).

[24] T. Zheleva, A. Lelis, G. Duscher, F. Liu, I. Levin, and M. Das, Appl. Phys. Lett. **93**, 022108 (2008).